

THE QUALITY OF THE ASCAT 12.5 KM WIND PRODUCT

Jur Vogelzang, Ad Stoffelen, Maria Belmonte, Anton Verhoef, and Jeroen Verspeek

Royal Netherlands Meteorological Institute, Wilhelminalaan 10, 3732 GK, De Bilt, The Netherlands

Abstract

The Advanced Scatterometer (ASCAT) delivers high resolution measurements of the ocean surface vector winds since 2006. Level 2 processing is done with the ASCAT Wind Data Processor (AWDP). AWDP builds upon the experience gained with the European scatterometers on board ERS-1 and ERS-2 as well as the U.S. SeaWinds scatterometer carried by QuikSCAT. It has several advanced features, in particular Two Dimensional Variational Ambiguity Removal (2DVAR). Operational wind products on a 12.5 km grid are produced since early 2009. In this contribution the quality of the 12.5 km ASCAT wind products is compared to that of other operational scatterometer wind products using buoy collocations and spectral techniques. Also the effect of level 1 processing is investigated. Some developments for the near future are briefly discussed.

1. INTRODUCTION

ASCAT carried by MetOp-A is a C-band scatterometer operated by the European METeorological SATellite organisation (EUMETSAT). Level 2 processing is done with AWDP. It builds upon the experience gained with the European scatterometers on board ERS-1 and ERS-2 as well as the U.S. SeaWinds scatterometer carried by QuikSCAT. AWDP has several advanced features, in particular Two Dimensional Variational Ambiguity Removal (2DVAR).

AWDP is developed in the framework of the Satellite Application Facility for Numerical Weather Prediction (NWP SAF). It can be obtained free of charge from the NWPSAF web site at www.nwpsaf.org. AWDP1.0 has been released on January 13, 2009. ASCAT wind products at 25 km and 12.5 km grid sizes are available from the Ocean and Sea Ice (OSI) SAF web site at www.osi-saf.org and www.knmi.nl/scatterometer. The 12.5 km ASCAT wind products are operational since March 3, 2009. A coastal wind product on a 12.5 km grid is foreseen to become operational in 2011 (*Portabella et al.*, 2008). Figure 1 shows an example of ASCAT's coverage over the globe in 24 hours. The OSI SAF web site also contains detail wind field images with wind arrows or wind flags, statistics of buoy comparisons for validation purposes, and comparisons to the ECMWF model winds for monitoring.

The general scheme of AWDP (or any other scatterometer wind processor) is shown in figure 2. The basic input data are the radar cross sections of the ocean surface measured by the scatterometer. In the inversion step these data are compared to a Geophysical Model Function (GMF), an empirical function that gives the radar cross section as a function of wind speed and wind direction, observation geometry and radar frequency and polarization. Figure 3 shows the GMF in measurement space for varying wind speed and direction. For ASCAT it has the shape of a folded cone with two sheets. In general, the inversion step returns two solutions. These so-called ambiguities have almost the same wind speed but different wind direction. They are points on each of the two sheets of the GMF with (local) minimum distance to the observation point.

After quality control (detection and removal of cells with variable sea conditions, rain, sea ice, etc.), the ambiguities and their a priori probabilities can be fed into the data assimilation part of a Numerical Weather Prediction (NWP) model. If, on the other hand, the AWDP output is to be used as a stand alone product for nowcasting or oceanographic applications, the most likely solution must be found in the Ambiguity Removal step. AWDP uses a variational approach called Two Dimensional Variational Ambiguity Removal (2DVAR).

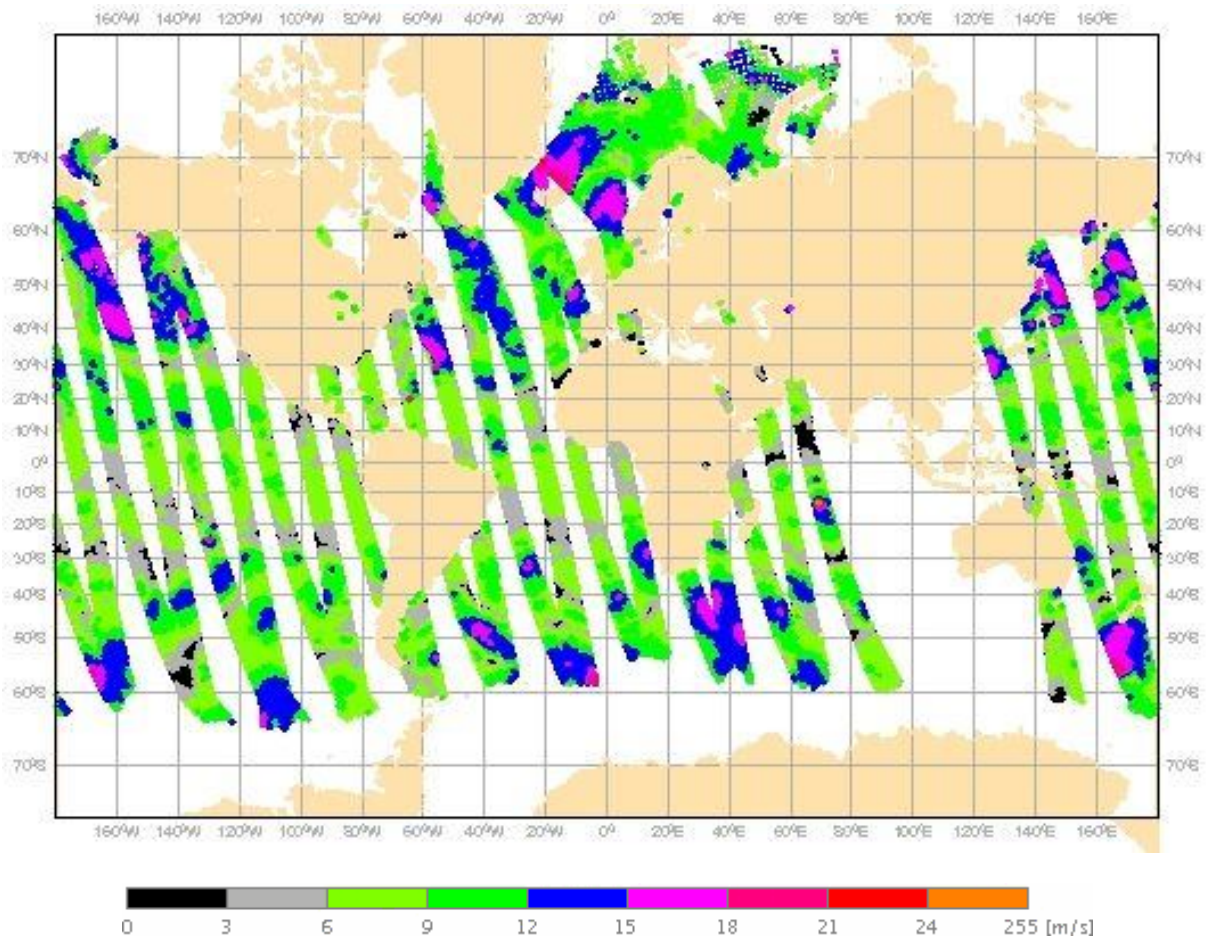


Figure 1: Global ASCAT coverage for November 16, 2009 as obtained from the OSI SAF web site. The colours indicate the wind speed. Only the ascending passes are shown.

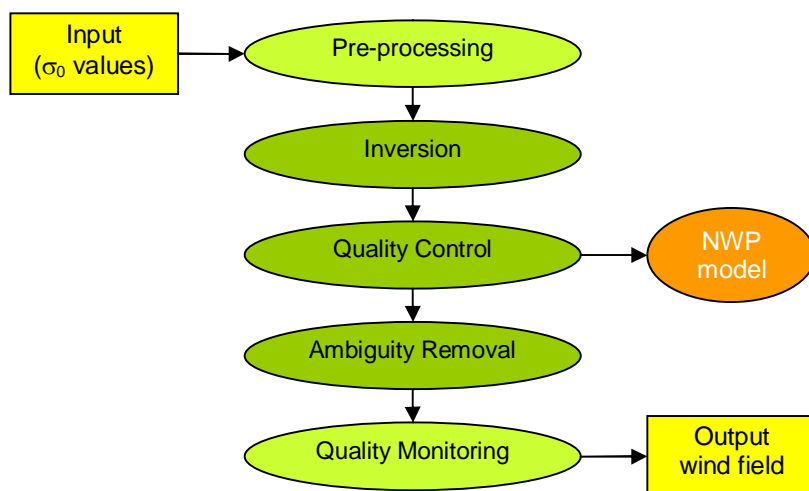


Figure 2: General scheme of scatterometer processing.

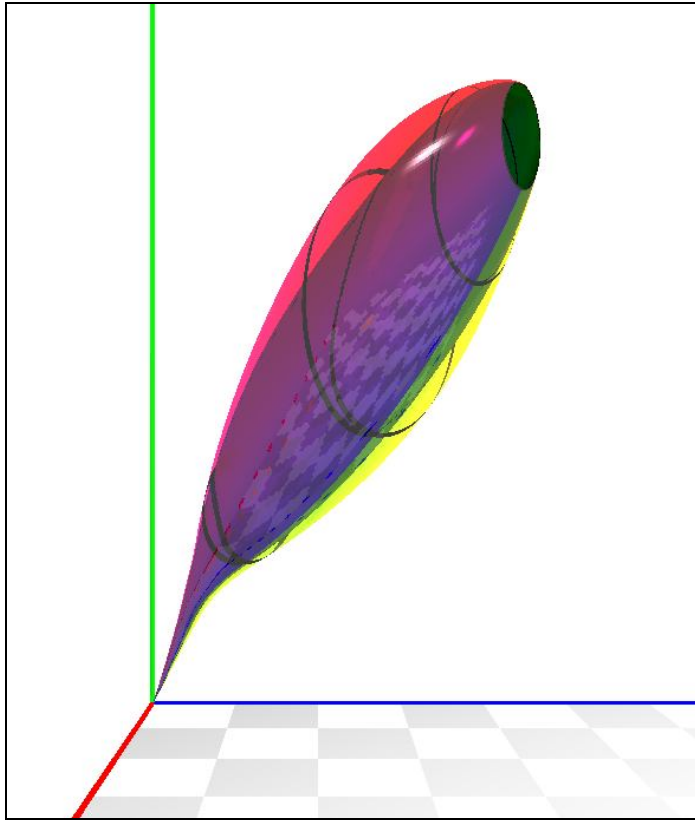


Figure 3: Impression of the Geophysical Model Function CMOD5.N. The axes denote the radar cross section for the forward beam (red), the mid beam (green) and the aft beam (blue). The wind speed varies along the cone, ranging from 0 to 40 m/s with a black band at every 10 m/s. The wind direction is given by the color of the cone..

2DVAR makes an analysis of the scatterometer observations and a background wind field, taking the a priori probabilities and physical laws into account. Next, the ambiguity closest to the analysis is selected as solution. In this way, 2DVAR leads to both statistically and physically consistent wind fields (Vogelzang *et al.*, 2009).

In an earlier contribution (Vogelzang *et al.*, 2008) the quality of ASCAT wind fields with 25 km and 12.5 km grid size was studied by estimating the amount of observation noise, by comparison with ECMWF model calculations, and by studying the selection probabilities and flag setting frequencies. It was a.o. concluded that the observation noise estimates show no significant white noise floor in the ASCAT wind products and that the 12.5 km product compares well with the 25 km product.

This contribution focuses on the 12.5 km product, in particular on buoy comparison and the effect of level 1 processing, i.e., the method of averaging individual measurements of the radar cross section. Finally a new model for sea ice detection is presented.

2. BUOY COMPARISON

Table 1 shows the buoy comparison of several operational scatterometer wind products: the ASCAT products on 12.5 km and 25 km grid size, as obtained from the OSI SAF web site and the SeaWinds product on a 25 km grid as obtained from the OSI SAF web site (labelled "KNMI") and the SeaWinds 25 km product disseminated by the National Oceanic and Atmospheric Administration, labelled "NOAA". Table 1 is based on collocated data from October 2008 with all buoys that are not blacklisted by the European Centre for Medium-Range Weather Forecasts (ECMWF). These buoys are mainly in the Tropics and near the coast of Europe and North America. Observations are considered as collocated when their time difference is 30 minutes at most and their spatial distance less than the scatterometer grid size divided by the square root of two.

ASCAT 12.5		ASCAT 25		SeaWinds 25 KNMI		SeaWinds 25 NOAA	
σ_u	σ_v	σ_u	σ_v	σ_u	σ_v	σ_u	σ_v
1.67	1.65	1.70	1.64	1.76	1.83	2.19	1.99

Table 1: Standard deviation of the difference between collocated buoy and scatterometer measurements for October 2008.

Table 1 shows that the ASCAT 12.5 km product compares slightly better with the buoys than the 25 km product. This is because the scatterometer gives the average wind over an area, while the buoy measures at a single point. The buoy winds therefore contain more variance than the scatterometer winds, resulting in a representation error that decreases with decreasing scatterometer footprint. Note also that the ASCAT results compare better with buoys than those of SeaWinds. This is due to ASCAT's more favourable measurement geometry that minimizes instrumental noise. As was shown earlier (*Vogelzang et al., 2009*) KNMI's wind product from SeaWinds data contains less noise than NOAA's, resulting in a better comparison with buoy data.

Figure 4 shows the spectra of the zonal and meridional wind components, u (left hand panel) and v (right hand panel) for the wind products in table 1 (green curves for ASCAT, blue curves for SeaWinds), together with the ECMWF model wind spectra (red curves). The spectra were obtained using samples of 128 consecutive wind vectors. Isolated missing values were linearly interpolated. Though the sample length is typically 3200 km (1600 km for ASCAT 12.5 km winds), there are still variations in the wind at scales larger than the sample length. These were removed by high pass

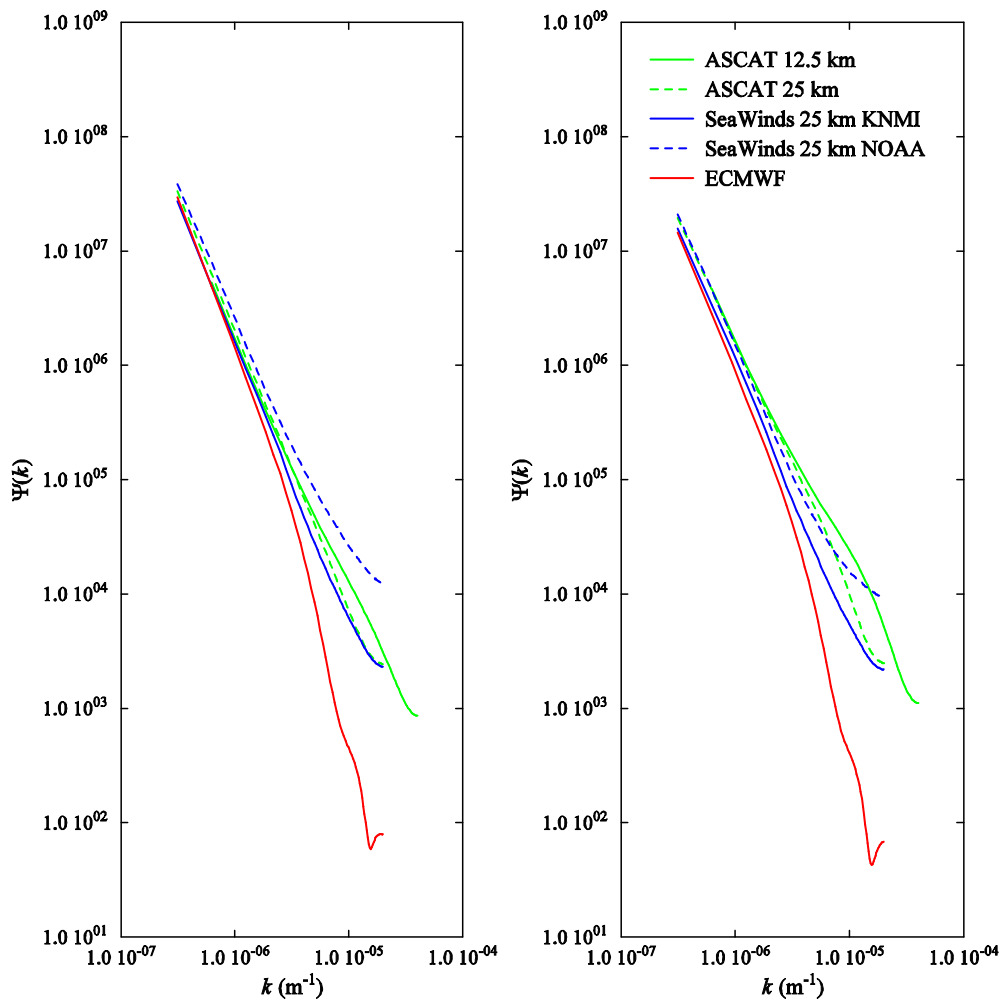


Figure 4: Spectra for the wind components u (left) and v (right) for ASCAT (green curves), SeaWinds (blue curves) and the ECMWF model (red curves).

filtering each sample with the first difference method before the FFT operation and correcting the resulting spectrum with the first difference transfer function (*Percival and Walden, 1992*). The spectra are normalized such that its integral over all positive values of the spatial frequency k equals the total variance.

Figure 4 shows that the ASCAT 12.5 km product (solid green curves) contains more small scale information than the 25 km product (dashed green curves). This is easily understood when viewing the scatterometer winds as a spatial average: the smaller the averaging area, the more variability in the wind.

Figure 4 also shows that the spectra of NOAA's SeaWinds wind product tend to become horizontal at high spatial frequencies (small spatial scales), especially for the meridional wind component v . This is considered as a manifestation of the noise floor in the NOAA SeaWinds 25 km wind product, the level of which was estimated in nadir view to be about 1.5 m/s for u and about 1 m/s for v (*Vogelzang et al., 2009*). The ASCAT spectra show no sign of such a noise floor except at the highest spatial frequencies. The ASCAT 25 km product contains slightly more signal at small scale than KNMI's SeaWinds 25 km product, notably for the meridional wind speed v . Note the rapid cut-off at small scales in the ECMWF model winds (red curves). Such reduced small-scale variability arguably improves medium-range weather predictability.

3. LEVEL 1 PROCESSING

During level 1 ASCAT processing the individual radar measurements are gridded to average cross sections that can be handled by AWDP. In order to minimise noise, a Hamming window is applied as indicated in figure 5. Note that figure 5 pertains to a grid size of 25 km; for a grid size of 12.5 km all sizes have to be divided by 2. The result of this procedure is that the effective resolution decreases: the ASCAT 25 km products are based on weighted radar cross section averages over an area of 100 km by 100 km with a resolution of 50 km. The main contribution, of course, originates from the central area measuring 50 km by 50 km that is shown in grey in figure 5.

One would expect that box averaging, i.e., averaging only over the grey area in figure 5.4, would result in more small scale details, but possibly at the expense of some noise. EUMETSAT has processed the ASCAT data from the period December 17, 2008 to January 11, 2009 using this box averaging.

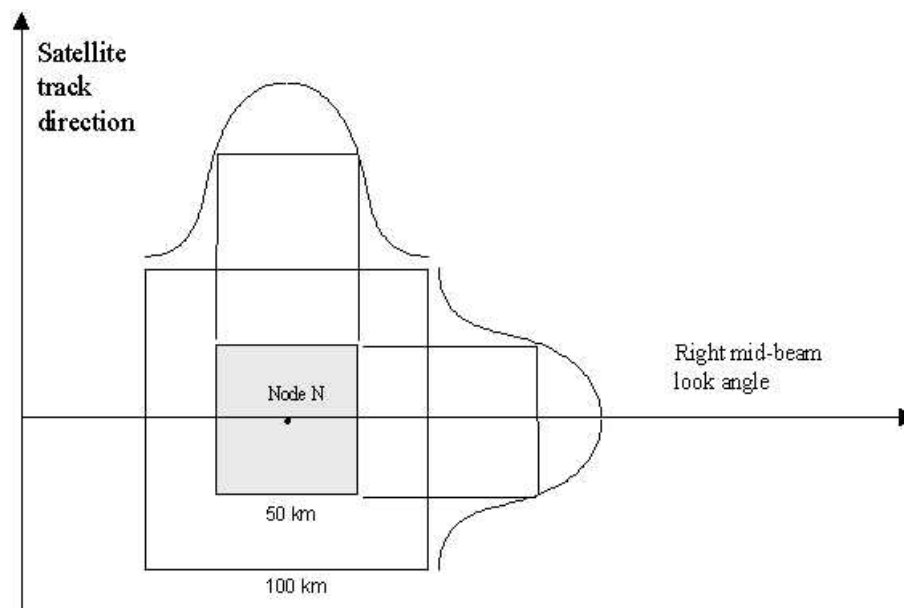


Figure 5: Level 1 processing grid definition (courtesy EUMETSAT).

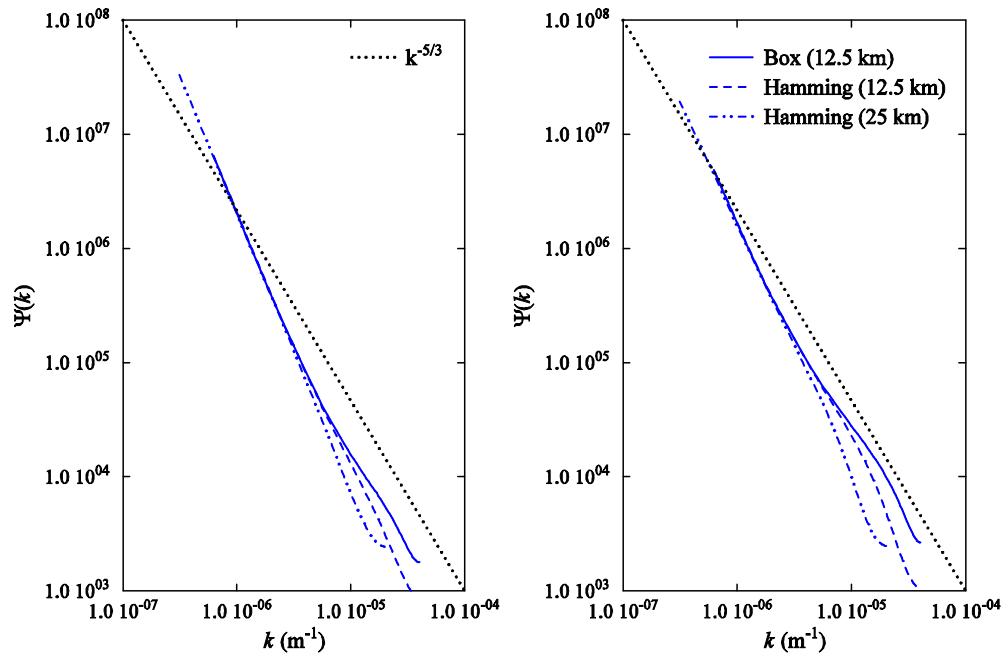


Figure 6: ASCAT spectra for the meridional wind components u (left) and v (right) for box averaging in level 1 processing at 12.5 km (solid curves) and for the standard level 1 processing at 12.5 km (dashed curves) and 25 km (dot-dashed curves). The dotted lines show a $k^{-5/3}$ spectrum.

The spectra in figure 6, based on all data from this period, confirm that the box averaging indeed leaves more small scale details in the retrieved wind fields, without any sign of increased instrumental noise. Moreover, the box-averaged spectrum at small scales (of the order of 100 km) falls off with an exponent near $-5/3$, the value predicted from Kolmogorov's turbulence theory and found from aircraft measurements, see e.g. (*Nastrom and Gage, 1985*). The Hamming-averaged spectra fall off steeper with an exponent of about -2 , a value found in earlier studies, e.g., (*Freilich and Chelton, 1986*).

4. SEA ICE MODEL

A new sea ice model has been developed for ASCAT. It is based on a Bayesian approach using Geophysical Model Functions (GMF) for wind and for sea ice. Figure 2 already showed the GMF for wind. The GMF for ice has the shape of a line that appears right under the wind cone. At high winds the ice GMF may cross the wind GMF, which complicates the water/ice classification procedure. The same approach was also applied to SeaWinds, and some general information on the method can be found in (*Belmonte Rivas and Stoffelen, 2009*).

Figure 7 gives two examples of the sea ice model over Antarctica in 2008: one during the minimum sea ice extent in April (left hand panel) and the other during the maximum sea ice extent in October (right hand panel). The ASCAT sea ice model is currently being tuned and is planned to become part of AWDP in the near future.

5 CONCLUSIONS

The ASCAT Wind Data Processor (AWDP) processes the level 1 ASCAT data into a level 2 wind product. Operational wind products on 25 km and 12.5 km grid size are disseminated and presented on the OSI SAF web site at www.osi-saf.org and www.knmi.nl/scatterometer. The AWDP software can be obtained free of charge from the NWPSAF web site at www.nwpsaf.org.

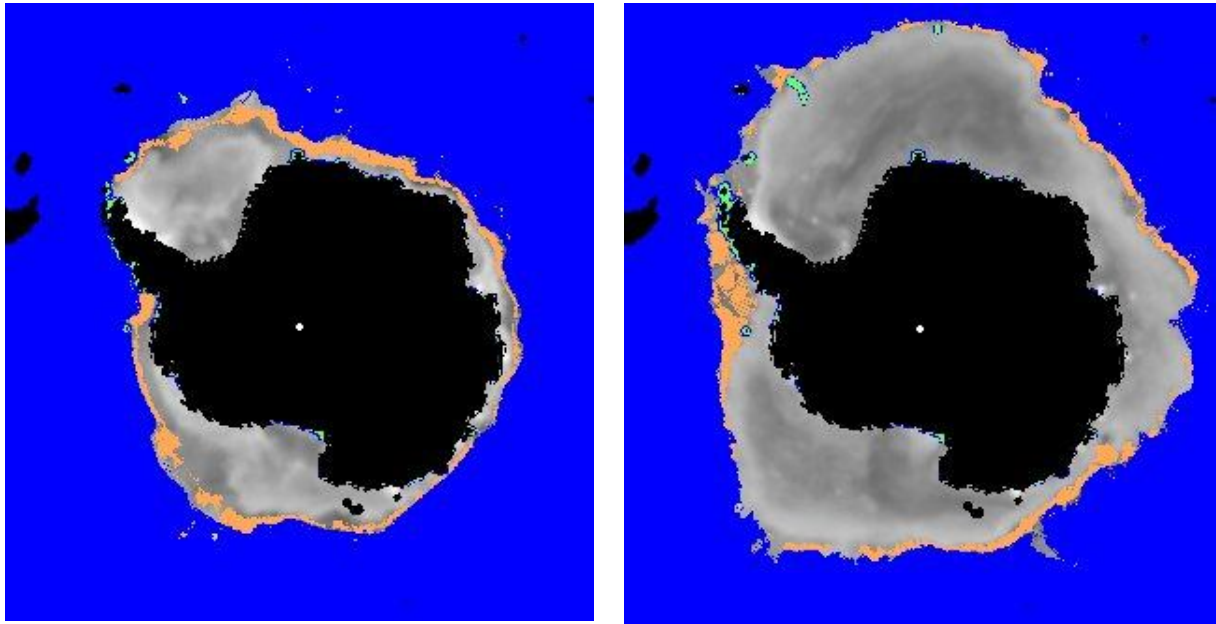


Figure 7: Results for the ASCAT sea ice model over Antarctica in April 2008 (left) and October 2008 (right)

The ASCAT winds compare well with collocated buoy measurements. The ASCAT 25 km product compares better to buoy observations than operational SeaWinds 25 km products. The ASCAT 12.5 km product contains more small scale information than the 25 km products. This is confirmed by spectral analysis of the scatterometer wind products. Small scales in the 12.5 km product are even preserved better when during level 1 processing the averaged radar cross sections are obtained by box averaging rather than standard Hamming window averaging. Moreover, such processing provides many more winds in coastal areas and a box-averaged product is being developed for this reason.

Further improvement of the ASCAT winds can be expected from the new sea ice model that is currently being tuned.

ACKNOWLEDGEMENTS

The authors wish to acknowledge EUMETSAT, in particular Julia Figa, for making available the box-averaged level 1 ASCAT data and Jean Bidlot at ECMWF for providing the buoy winds.

REFERENCES

- Belmonte Rivas, M. and A. Stoffelen (2009) A Bayesian sea ice detection algorithm for QUIKSCAT. Submitted to *IEEE Trans. Geoscience and Rem. Sens.*
- Freilich, M.H., and D.B. Chelton, wavenumber spectra of Pacific winds measured by the Seasat scatterometer. *J. Phys. Ocean.* 16, 741-757.
- Nastrom, G.D., and K.S. Gage (1985) A climatology of atmospheric wavenumber spectra of wind and temperature observed by commercial aircraft. *J. Atmos. Sci.* 42, 950-960.
- Percival, D.B., and A.T. Walden (1993) *Spectral analysis for physical applications*. Cambridge University Press, Cambridge, New York, U.S.A.
- Portabella, M., A. Stoffelen, M. Belmonte, A. Verhoef, J. Verspeek, and J. Vogelzang (2008) High resolution ASCAT scatterometer winds near the coast. *Proc. 2008 EUMETSAT Meteorological satellite Conference, Darmstadt, Germany, 8-12 September 2008, EUMETSAT P.52*. Available from

www.eumetsat.int/Home/Main/AboutEUMETSAT/Publications/ConferenceandWorkshopProceedings/2008/SP_1232700911980?l=en.

Vogelzang, J., A. Stoffelen, M. Belmonte, M. Portabella, A. Verhoef, and J. Verspeek (2008) Quality of high resolution ASCAT wind fields. *Proc. 2008 EUMETSAT Meteorological satellite Conference, Darmstad, Germany, 8-12 September 2008, EUMETSAT P.52*. Available from www.eumetsat.int/Home/Main/AboutEUMETSAT/Publications/ConferenceandWorkshopProceedings/2008/SP_1232700911980?l=en.

Vogelzang, J., A. Stoffelen, A. Verhoef, J. de Vries, and H. Bonekamp (2009) Validation of two-dimensional variational ambiguity removal on SeaWinds scatterometer data. *J. Atm. Ocean. Tech.* 1229-1245.